Dimensional and hydrodynamic properties of amylose tris(phenylcarbamate) in various solvents

2009 J. Phys.: Conf. Ser. 184 012006

(http://iopscience.iop.org/1742-6596/184/1/012006)

Journal of Physics: Conference Series **184** (2009) 012006 doi:10.1088/1742-6596/184/1/012006

Dimensional and hydrodynamic properties of amylose tris(phenylcarbamate) in various solvents

Ken Terao

Department of Macromolecular Science, Osaka University, 1-1 Machikaneyama-cho, Toyonaka, Osaka 560-0043, Japan

E-mail: kterao@chem.sci.osaka-u.ac.jp

Abstract. Analyzes were made of the particle scattering function $P(k)$, z-average radii of gyration and intrinsic viscosities for amylose tris phenylcarbamate samples having different weight-average molecular weight M_w in 1,4-dioxane (DIOX), 2-ethoxyethanol (2EE), methyl acetate and 4-methyl-2-pentanone at 25 °C and in ethyl acetate at 33°C, on the basis of the wormlike cylinder model with or without excluded volume to determine the contour length per residue h and the Kuhn segment length. The h values in a ketone and esters were found to be significantly larger than those in DIOX and 2EE. Furthermore, the discrepancy between the experimental $P(k)$ for an ATPC sample (M_w = 18700) and the theoretical values at high k (absolute value of the scattering vector) region (k > 3 nm^{-1}) became more significant with decreasing h, suggesting that the $P(k)$ data at the k region reflect the helical structure of the polymer.

1. Introduction

In crystal structure, varieties of conformations having different helical pitch per residue h were found for amylosic chains; indeed, this h for amylose triesters ranges from 0.37 to 0.40 nm [1]. This indicates that the small perturbation (e.g. side chains and solvents) to the amylosic main chain may influence the local conformation and then h of amylosic chains in solution.

Much work has been done for dimensional and hydrodynamic properties of amylose tris phenylcarbamate (ATPC), whose chemical structure is shown in Figure 1, in solution [2–13]. This polymer has three pairs of polar NH and C=O groups. The above mentioned feature of amylosic chains suggests that h could depend on polar solvents having different chemical structure. However, we find only a few reports of h in solution. Thus we recently undertook studies on solution properties

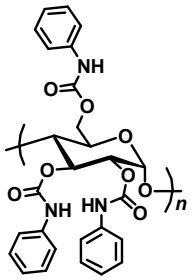

Figure 1. Chemical structure of amylose tris phenylcarbamate (ATPC).

of ATPC samples synthesized from enzymatically synthesized amylose [14]. To determine the weight-average molecular weight M_w, the z-average mean square radius of gyration $<S^2>_z$, the particle scattering function $P(k)$ and the intrinsic viscosity $[\eta]$, where k denotes the magnitude of the scattering vector, light and synchrotron radiation small-angle X-ray scattering (SAXS) and viscosity measurements were made on the ATPC samples in 1,4-dioxane (DIOX), 2-ethoxyethanol (2EE), methyl acetate (MEA), ethyl acetate (EA) and 4-methyl-2-pentanone (MIBK). The obtained ratios of M_w to the number-average molecular weight or those of the z-average molecular weight to M_w were about 1.1 or less [15]. We made the measurements at 25 °C for DIOX, 2EE, MEA and MIBK solutions whereas 33 °C for the rest because it was determined to be the theta temperature. It is expected that carbonyl groups of ketones and esters may form hydrogen bonding with NH groups of ATPC, thus the solvent dependence in the local conformation of ATPC could be detectable as the difference of h.

This paper abstracts the major results from our recent analyses [15, 16] of the solution data for ATPC in terms of the Kratky-Porod (KP) wormlike chain model [17] and the possibility to estimate the local conformation of the polymer in solution from scattering data.

2. Results and discussion

2.1. Analysis in terms of the KP chain

Figure 2 shows the molecular weight dependence of $<S^2>_z$ for ATPC in DIOX [15] and MIBK [16] at 25 °C. The discrepancy of $<S^2>_z$ in the two solvents becomes more significant with decreasing M_w, indicating unmistakable difference of M_L (molar mass per unit contour length). The obtained $<S^2>_z$, $P(k)$ and $[\eta]$ data in the five solvents were analyzed by the known theories [18, 19] for the KP chain model with excluded volume to determine M_L, λ^{-1}, the chain diameter d and the excluded-volume strength B; we note that one or two parameters of $[\eta]$ were assumed because all parameters cannot uniquely be determined. The theoretical solid curves for $<S^2>_z$ (Figure 2) and $[\eta]$ (Figure 3) reproduce the corresponding experimental data almost quantitatively. Furthermore, the experimental

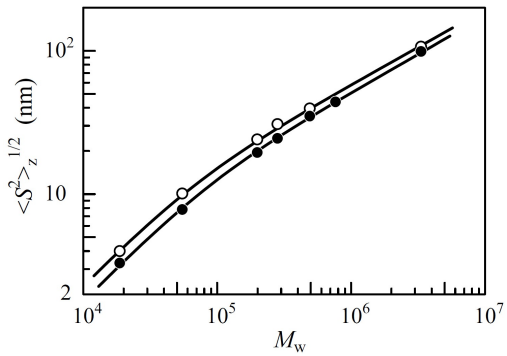

Figure 2. Molecular weight dependence of $<S^2>_z^{1/2}$ for ATPC in DIOX (filled circles) [15] and MIBK (open circles) [16] at 25 °C. Solid curves, theoretical values for the perturbed wormlike chains with M_L = 1550 nm^{-1}, λ^{-1} = 24 nm, B = 1 nm in DIOX and M_L = 1190 nm^{-1}, λ^{-1} = 24 nm, B = 0.5 nm in MIBK.

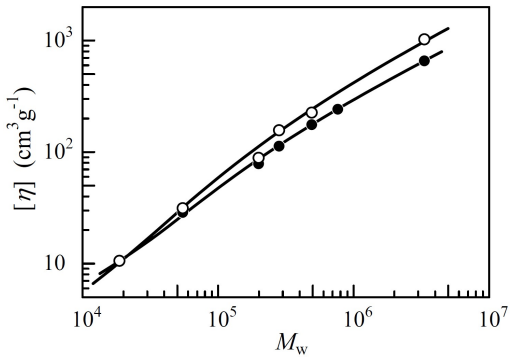

Figure 3. Molecular weight dependence of $[\eta]$ for ATPC in DIOX (filled circles) [15] and MIBK (open circles) [16] at 25 °C. Solid curves, theoretical values for the perturbed wormlike cylinders with M_L = 1540 nm^{-1}, λ^{-1} = 20 nm, d = 2.9 nm and B = 0.5 nm in DIOX and M_L = 1310 nm^{-1}, λ^{-1} = 23.5 nm, d = 1.9 nm and B = 0.5 nm in MIBK.

$P(k)$ for an ATPC sample (ATPC20K, $M_w = 1.87 \times 10^4$) is also fitted by the corresponding theoretical $P(k)$ in the range of $k < 3$ nm^{-1} (Figure 4); the discrepancy between the theoretical and experimental $P(k)$ in high k region reflects the local atomic structure of ATPC in solution. The molecular parameters obtained from the three different physical properties substantially agree within the possible experimental and determination errors other than d in DIOX; this inconsistency suggests the d value from SAXS can be affected by the electron density profile around the chain contour [18, 20]. The resultant λ^{-1} and h (contour length per repeat unit) calculated from $h = M_0/M_L$ (M_0: molar mass per repeat unit) are summarized in Table 1.

2.2. Solvent dependence of local chain length

The h values in DIOX and 2EE are significantly larger than those in a ketone and esters; i.e. h in MIBK is about 30% longer than that in 2EE, showing that the local conformation of ATPC significantly depends on the solvent. This behaviour is most likely due to the difference in the hydrogen bonding between intramolecular NH and C=O groups and intermolecular hydrogen bonding between the polar groups of ATPC and solvent molecules. We note that the intramolecular hydrogen bonding of ATPC in DIOX and 2EE was observed as splitting amide I band in their solution IR spectra [15]. We may thus speculate that the intramolecular hydrogen bonding is replaced in ketones and esters by the intermolecular hydrogen bonding between the NH groups of ATPC and the C=O groups of the solvent molecules, and then the main chain of ATPC extends. Slightly increase both h and λ^{-1} with molar volume of the solvent (MEA < EA < MIBK) seems to be consistent with this suggestion when we consider the hydrogen bonding solvent molecules instabilize the conformation

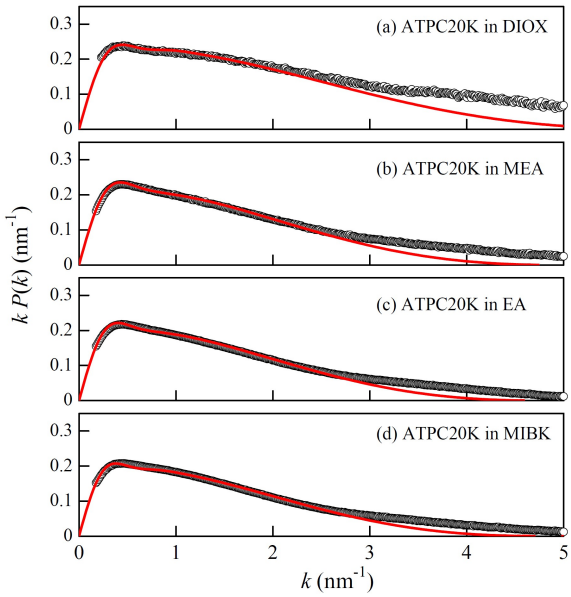

Figure 4. Holtzer plots for ATPC20K ($M_w = 1.87 \times 10^4$) in DIOX at 25 °C, MEA at 25 °C, EA at 33 °C, MIBK at 25 °C. Solid curves, theoretical values for the wormlike cylinder with $M_L = 1500$ nm^{-1}, $\lambda^{-1} = 21$ nm, $d = 1.3$ nm in DIOX, $M_L = 1380$ nm^{-1}, $\lambda^{-1} = 14$ nm, $d = 1.6$ nm in MEA, $M_L = 1310$ nm^{-1}, $\lambda^{-1} = 16$ nm, $d = 1.6$ nm in EA and $M_L = 1270$ nm^{-1}, $\lambda^{-1} = 23$ nm, $d = 1.6$ nm in MIBK. (The data in the range of $k < 2.5$ nm^{-1} have been published in refs [15, 16]).

Table 1. Comparison of h and λ^{-1} for ATPC in Various Solvents.

Solvent	T (°C)	h (nm)	λ^{-1} (nm)
2EE [a]	25	0.32 ± 0.01	16 ± 2
DIOX [a]	25	0.34 ± 0.01	22 ± 2
MEA[b]	25	0.37 ± 0.02	15 ± 2
EA[b]	33	0.39 ± 0.02	17 ± 2
MIBK[b]	25	0.42 ± 0.02	24 ± 2

[a] Reference [15]. [b] Reference [16].

having short helical pitch. However, no spectroscopic evidence has been obtained for either intra- or intermolecular hydrogen bonding in ketones and esters because of inapplicability of either FT-IR or circular dichroism measurements. Investigation of appropriate amylose derivative-solvent systems could be useful to clarify solvent dependent local conformational behaviour of amylosic chains.

2.3. Scattering data at high k range

The discrepancy between theoretical and experimental scattering function in Figure 4 occurs at the region $k > 3$ nm^{-1}, indicating that the continuous cylinder model should not be applicable to the data there. Interestingly, the difference increases with decreasing h. This is reasonable when we consider the higher scattering intensity than the theoretical value reflects the local helical structure which becomes more appreciable with shortening h. Thus, the analyses of $P(k)$ at high k range are probably useful to determine the local conformational features of amylose derivatives in solution. However, the scattering function at the k range is generally affected by the local conformational fluctuation and the electron density profiles of solvent molecules around the polymers chains [20]; the former probably weakens the characteristic peaks. Therefore, no further analysis is made at the present time due to the difficulty of the estimation of each effect on $P(k)$. We may conjecture that the comparison between the atomic structure generated by molecular simulation and the accurate and wide-range experimental scattering functions is helpful to obtain new insights for the local conformation of the polymers in solution.

Acknowledgements

The author thanks Prof. T. Norisuye, Prof. T. Sato (Osaka University) and Prof. S. Kitamura (Osaka Prefecture University) for fruitful discussions. The synchrotron radiation experiments were performed at the BL40B2 in SPring-8 with the approval of the Japan Synchrotron Radiation Research Institute (JASRI) (Proposal #2007A1034, #2007B1296 and #2008A1313).

References

[1] Zugenmaier P and Steinmeier H 1986 *Polymer* **27** 1601
[2] Burchard W 1964 *Z. Physik. Chem.* **42** 293
[3] Cowie J M G 1965 *Biopolymers* **3** 69
[4] Burchard W 1965 *Makromol. Chem.* **88** 11
[5] Banks W, Greenwood C T and Sloss J 1970 *Makromol. Chem.* **140** 109
[6] Banks W, Greenwood C T and Sloss J 1970 *Makromol. Chem.* **140** 119
[7] Banks W and Greenwood C T 1971 *Makromol. Chem.* **144** 135
[8] Banks W, Greenwood C T and Sloss J 1971 *Eur. Polym. J.* **7** 879
[9] Burchard W 1971 *Br. Polym. J.* **3** 214
[10] Sutter W and Burchard W 1978 *Makromol. Chem.* **179** 1961
[11] Gupta A K, Marchal E, Burchard W and Pfannemüller B 1979 *Macromolecules* **12** 281
[12] Pfannemüller B, Schmidt M, Ziegast G and Matsuo K 1984 *Macromolecules* **17** 710
[13] Muroga Y, Hayashi K, Fukunaga M, Kato T, Shimizu S and Kurita K 2006 *Biophys. Chem.* **121** 96
[14] Kitamura S, Yunokawa H, Mitsuie S and Kuge T 1982 *Polym. J.* **14** 93
[15] Terao K, Fujii T, Tsuda M, Kitamura S and Norisuye T 2009 *Polym. J.* **41** 201
[16] Fujii T, Terao K, Tsuda M, Kitamura S and Norisuye T 2009 *Biopolymers* in press DOI: 10.1002/bip.21219
[17] Kratky O. and Porod G 1949 *Recl. Trav. Chim. Pays-Bas* **68** 1106
[18] Yamakawa H 1997 *Helical Wormlike Chains in Polymer Solutions* (Berlin: Springer)
[19] Nakamura Y and Norisuye T 2004 *J. Polym. Sci. B: Polym. Phys*. **42** 1398
[20] Terao K, Mizuno K, Murashima M, Kita Y, Hongo C, Okuyama K, Norisuye T and Bächinger H P 2008 *Macromolecules* **41** 7203